

## Anomalous properties and the liquid-liquid phase transition in gallium

Renzhong Li, Gang Sun, and Limei Xu\*

Citation: *J. Chem. Phys.* **145**, 054506 (2016); doi: 10.1063/1.4959891

View online: <http://dx.doi.org/10.1063/1.4959891>

View Table of Contents: <http://aip.scitation.org/toc/jcp/145/5>

Published by the [American Institute of Physics](#)

---

### Articles you may be interested in

[The phase behavior study of human antibody solution using multi-scale modeling](#)

*J. Chem. Phys.* **145**, 194901194901 (2016); 10.1063/1.4966972

[Relationship between the potential energy landscape and the dynamic crossover in a water-like monatomic liquid with a liquid-liquid phase transition](#)

*J. Chem. Phys.* **146**, 014503014503 (2017); 10.1063/1.4973348

---



**COMPLETELY  
REDESIGNED!**

**PHYSICS  
TODAY**

*Physics Today* Buyer's Guide  
Search with a purpose.

# Anomalous properties and the liquid-liquid phase transition in gallium

Renzhong Li,<sup>1</sup> Gang Sun,<sup>1</sup> and Limei Xu<sup>1,2,a)</sup>

<sup>1</sup>International Center for Quantum Materials and School of Physics, Peking University, Beijing 100871, China

<sup>2</sup>Collaborative Innovation Center of Quantum Matter, Beijing, China

(Received 20 April 2016; accepted 14 July 2016; published online 3 August 2016)

A group of materials including water and silicon exhibit many anomalous behaviors, e.g., density anomaly and diffusivity anomaly (increase upon compression). These materials are hypothesized to have a liquid-liquid phase transition (LLPT) and the critical fluctuation in the vicinity of the liquid-liquid critical point is considered as the origin of different anomalies. Liquid gallium was also reported to have a LLPT, yet whether it shows similar water-like anomalies is not yet studied. Using molecular dynamics simulations on a modified embedded-atom model, we study the thermodynamic, dynamic, and structural properties of liquid gallium as well as its LLPT. We find that, similar to water-like materials predicted to have the LLPT, gallium also shows different anomalous behaviors (e.g., density anomaly, diffusivity anomaly, and structural anomaly). We also find that its thermodynamic and structural response functions are continuous and show maxima in the supercritical region, the loci of which asymptotically approach to the other and merge to the Widom line. These phenomena are consistent with the supercritical phenomenon in a category of materials with a liquid-liquid critical point, which could be common features in most materials with a LLPT. *Published by AIP Publishing.* [<http://dx.doi.org/10.1063/1.4959891>]

## I. INTRODUCTION

Most substances have only one liquid, but there are some predicted to have two distinct liquid states,<sup>1–7</sup> a low-density liquid (LDL) and a high-density liquid (HDL), such as water,<sup>1</sup> phosphorus,<sup>2</sup> silicon,<sup>3</sup> and silica.<sup>4</sup> These substances exhibit similar anomalous behaviors, such as density anomaly,<sup>7–9</sup> thermodynamic anomaly,<sup>8–10</sup> and diffusivity anomaly.<sup>5,11</sup> The origin of such a phenomenon has been attracting extensive attentions and different scenarios have been proposed.<sup>12–14</sup> One scenario is the liquid-liquid critical point (LLCP) hypothesis, which suggests the existence of a first-order liquid-liquid phase transition (LLPT) terminating at a LLCP. According to this hypothesis, the critical fluctuations of the LLCP are considered as the origin of different anomalies.<sup>15–23</sup> In most cases, the predicted LLCP is buried in deep supercooled region where crystallization is unavoidable<sup>1–7</sup> or located at very high pressure where current experimental techniques are difficult to detect.<sup>24–26</sup> Thus, direct experimental confirmation of a LLCP, except in Y<sub>2</sub>O<sub>3</sub>-Al<sub>2</sub>O<sub>3</sub><sup>27</sup> and phosphorus,<sup>2</sup> is rare and challenging, even though the LLPT was reported in many theoretical and computational studies.<sup>1–7,24–26</sup>

Elementary gallium is another interesting substance that shares some common features with water, e.g., having multi-solid phases and negatively sloped melting line.<sup>28–34</sup> Tien *et al.*<sup>35</sup> observed two separate peaks at 260 K and 220 K in the nuclear magnetic resonance (NMR) spectra of opal-confined gallium which is interpreted as the existence of two liquid gallium phases confined in opal. Using computer simulations, Jara *et al.*<sup>36</sup> reported that gallium has two states of liquid,

the LDL and the HDL, and also estimated the LLCP of the LLPT between two liquid states. Cahuaranga *et al.*<sup>37</sup> investigated the dynamics of liquid gallium and found that the mobility of two liquids is different, higher in the HDL than that in the LDL. All these are indicative of a LLPT in liquid gallium. As mentioned above, substances with LLPT show similar anomalous properties, the specific question of interest here is the correlation between LLPT and anomalous behaviors in gallium. That is, whether gallium belongs to the group of materials that has a predicted LLPT and shares similar anomalous behavior (thermodynamic, dynamic, and structural) as substances like water.

Using molecular dynamics simulations on a modified embedded atom model (MEAM), we study the LLPT of gallium by investigating its thermodynamic, dynamic, and structural properties. We find that liquid gallium also shows density anomaly, diffusivity anomaly, and structural anomaly, similar to water. We also find that the response functions of volume, enthalpy, and translational order parameter are continuous and show maxima in the supercritical region, the loci of which asymptotically approach to one line (also called the Widom line)<sup>18,22,38</sup> and converge to the critical point, same as substances with a LLCP. Considering the fact that these phenomena are observed in a category of materials with a liquid-liquid critical point such as water and silicon, these studies show that the anomaly behavior might be common features for systems with a LLCP and LLPT.

## II. METHODS

Our system consists of  $N = 1152$  gallium atoms in a cubic box. The atoms interact with each other via the modified embedded-atom model (MEAM), which is the

<sup>a)</sup> Author to whom correspondence should be addressed. Electronic mail: limei.xu@pku.edu.cn

modified version of embedded-atom model (EAM). For both potentials, the energy of a system includes both the pair interaction energy and the energy to embed an atom into the background electron density. These potentials are fitted predominantly to the results from density-functional theory (DFT) calculations with parameters determined by the generalized gradient approximation (GGA) calculations.<sup>39</sup> For EAM potential, the background electron density is given by a linear supposition of spherically averaged atomic electron densities, while for MEAM potential, the background electron density is given by an angular dependence supposition, which was found to be critical in explaining the behavior of complex crystal structures.<sup>40</sup> The MEAM potential reproduces many properties of gallium, e.g., phase stability at ambient pressure, elastic constants, thermal expansion, specific heat, diffusivity, viscosity, free surface stability, and relaxation are in close agreement with experiments.<sup>28,41,42</sup>

Standard molecular dynamics simulations are performed using LAMMPS<sup>43</sup> and periodic boundary conditions are applied. Based on the Nose-Hoover chain with temperature and pressure (damping parameters of 75 fs and 1 ps), we perform constant pressure and temperature (NPT-ensemble) as well as constant volume and temperature (NVT-ensemble) simulations to study the liquid-liquid phase transition and properties of liquid gallium. Each MD simulation lasts for 20-40 ns with an integration time step of 1 fs and all properties are measured in equilibrium states for temperatures investigated.

### III. RESULTS

#### A. Equation of states

The equation of state is presented in Figure 1. Each state point along all isochores is obtained in equilibrium liquid state using NVT-ensemble MD simulation. As temperature decreases, there exists a region where isochores intersect. At each intersecting point, the system has same pressure

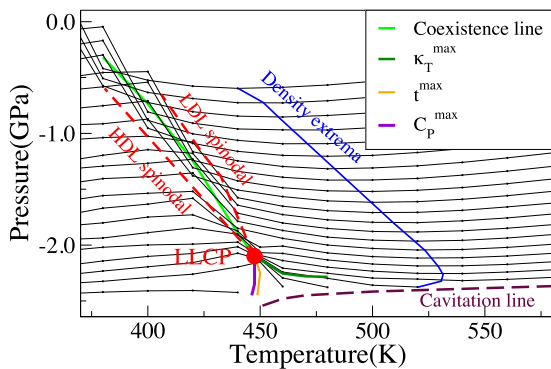


FIG. 1. The phase diagram of gallium. Isochores vary from  $V/N = 19.7, 19.8, 19.9, \dots, 21.9 \text{ \AA}^3$  (density from  $5.879 \text{ g/cm}^3$  to  $5.289 \text{ g/cm}^3$ ), indicated by the thin dotted lines. The spinodal lines (red line), the cavitation line (brown line), the coexistence line (green line), and the temperature of density extrema are also presented. The LLCP is located at  $T_C = 447.5 \text{ K}$  and  $P_C = -2.18 \text{ GPa}$  as the terminal point of coexistence line. We also present the thermodynamic anomaly, specific heat maximum  $C_P^{max}$  (purple line), the compressibility maximum  $\kappa_T^{max}$  (dark green line), and the response function maxima of the translational order parameter (orange line).

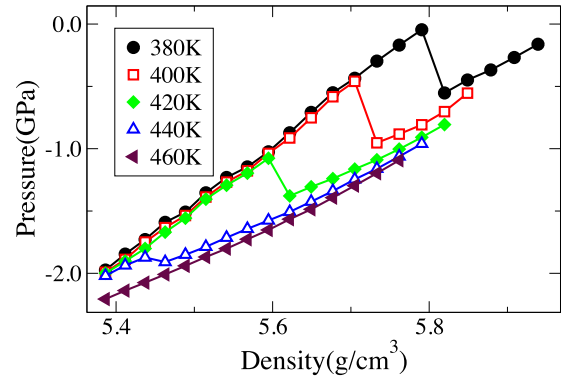


FIG. 2. The phase diagram in the P-V plane for temperatures ranging from 380 K to 450 K. The van der Waals loops for  $T < 450 \text{ K}$  are indicative of the existence of a first-order liquid-liquid phase transition.

and temperature but two different densities; thus, such intersections of isochores indicate the coexistence of two liquid states in liquid gallium. The first-order LLPT can also be confirmed from the van der Waals loop shown in Figure 2. Upon compression along isotherms, the LDL transforms to the HDL with a discontinuous change in volume for volume per atom larger than  $21.5 \text{ \AA}^3$  (density  $5.387 \text{ g/cm}^3$ ) above the cavitation line (Figure 1). The stability limit of the LDL and HDL, which are the spinodal lines of the LLPT, is determined by the highest and lowest crossings of isochores in the P-T phase diagram. The liquid-liquid coexistence region is in between the HDL and LDL spinodal lines. The slope of the LLPT coexistence line can be obtained by the Maxwell construction based on the van der Waals loop shown in Figure 2. Obviously, the coexistence line of liquid gallium is negatively sloped, similar to that of water. There are several ways to determine the LLCPC, e.g., the disappearance of hysteresis,<sup>36,44</sup> the crossing of isochores,<sup>44</sup> disappearing of van der Waals loop,<sup>44</sup> and extrapolating finite size critical parameters to the bulk critical values.<sup>45</sup> In this study, we determine the LLCPC as the lowest crossing point of isochores, located at  $T_C = 447.5 \pm 2.5 \text{ K}$ ,  $P_C = -2.15 \pm 0.05 \text{ GPa}$ , which is consistent with previous report in Ref. 36.

According to Clapeyron equation,

$$\frac{dP}{dT} = \frac{\Delta S}{\Delta V}, \quad (1)$$

where  $\Delta S$  is the entropy difference and  $\Delta V$  is the volume difference between LDL and HDL. Since the coexistence of two liquids is located in the density anomaly region,  $\Delta V$  is positive as temperature decreases. Therefore, the negative slope of the liquid-liquid coexistence indicates that the LDL has lower entropy thus more ordered than the HDL, same as that in water.

#### B. Density anomaly

According to general thermodynamic relation,

$$\left(\frac{\partial V}{\partial T}\right)_P = -\left(\frac{\partial P}{\partial T}\right)_V \left(\frac{\partial V}{\partial P}\right)_T, \quad (2)$$

and Maxwell relation,  $\left(\frac{\partial V}{\partial P}\right)_T = -V\kappa_T$ ,  $\left(\frac{\partial V}{\partial T}\right)_P = -V\kappa_T\left(\frac{\partial P}{\partial T}\right)_V$ , where  $\kappa_T$  is the isothermal compressibility. Since  $\kappa_T$  is

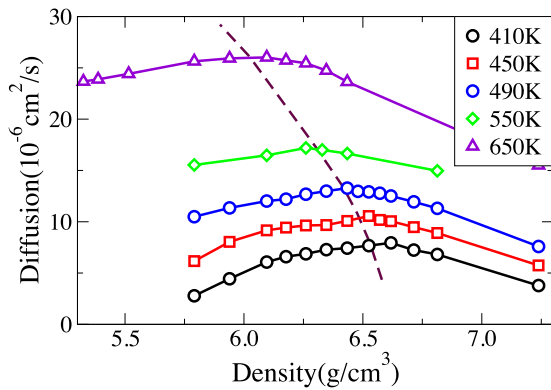


FIG. 3. The diffusion coefficient  $D$  along isotherms as a function of density. There exists a region where diffusivity increases upon compression along isotherms, indicative of diffusivity anomaly. The diffusivity extrema are denoted by dashed line.

always positive, the density extrema defined by  $(\frac{\partial V}{\partial T})_P = 0$  is equivalent to  $(\frac{\partial P}{\partial T})_V = 0$ , a minimum along isochore in the P-T phase diagram. Indeed, as shown in Figure 1, there exist minima along isochores for densities ranging from 5.28 g/cm<sup>3</sup> to 5.88 g/cm<sup>3</sup>, confirming the existence of density anomaly in liquid gallium. The loci of the temperature of maximum density (TMD) thus enclose the density anomaly region within which density decreases upon cooling along constant pressure (Figure 1).

### C. Diffusivity anomaly

We next study the dynamic properties of liquid gallium. For each state, we first calculate the mean-squared displacement  $\langle \bar{r}^2(t) \rangle$  and then use the Einstein relation to evaluate the diffusion coefficient,

$$D = \lim_{t \rightarrow \infty} \frac{\langle \bar{r}^2(t) \rangle}{6t}, \quad (3)$$

where  $\langle \dots \rangle$  denotes the average over all molecules and time origins. Figure 3 shows diffusivity  $D$  as a function of density. Along isotherms,  $D$  first increases and then exhibits a maximum as density increases. Such maximum along isotherms indicates the existence of diffusivity anomaly in liquid gallium, similar as that observed in liquid water and

water-like substances.<sup>7,44</sup> The diffusivity anomalous region is enclosed by the loci of diffusivity maxima,  $(\frac{\partial D}{\partial \rho})_T = 0$ , denoted by the  $D_{max}$  line shown in Figure 3.

### D. Structure anomaly

We next study the structural property of liquid gallium by investigating its translational order parameter  $t$ , defined as

$$t \equiv \int_0^{S_c} |g(s) - 1| ds, \quad (4)$$

where  $g(s)$  is the pair correlation function, and  $s \equiv rn^{1/3}$  is the radial distance scaled by the mean inter-particle distance. For random packing (e.g., gas phase)  $g = 1$ , thus  $t$  vanishes, while for ordered structure with long-range translational order (e.g., crystal),  $g \neq 1$  over long distance,  $t$  is nonzero. The result of  $t$  for different temperatures is presented in Figure 4(a). As can be seen,  $t$  is discontinuous for  $T < 450$  K and continuous for  $T > 450$  K. The discontinuity is consistent with a first-order LLPT in liquid gallium mentioned above. For higher temperatures,  $t$  first decreases and then shows a minimum upon compression [Fig. 4(b)], indicative of structure anomaly, also reported in SPC/E water.<sup>46</sup> We locate the minimum of translational order  $t$  upon compression along isotherms and the line of structural order anomaly (loci of  $t$  extrema) is presented in the P-T phase diagram of gallium in Figure 8.

We also study the structural property in terms of local packing (Fig. 5). We calculate the number of nearest neighbors ( $nn$ ) of atoms in two liquids by integrating the pair correlation function  $g(r)$  from  $r = 0$  to  $r_{min}$  chosen as the distance of the first minimum of pair correlation function  $g(r)$ . The atoms typically have 9 nearest neighbors for the HDL, while it is 8 for the LDL.<sup>36</sup> We classify each atom by the number of its nearest neighbors ( $nn$ ) as HDL-like if  $nn \geq 9$  and LDL-like if  $nn < 9$ . The population of HDL-like atoms decreases while the population of LDL-like atoms increases as temperature decreases, which is consistent with previous results reported in Ref. 36.

### E. Response functions

We further investigate the response functions beyond the LLCP in the supercritical region. The state functions, such

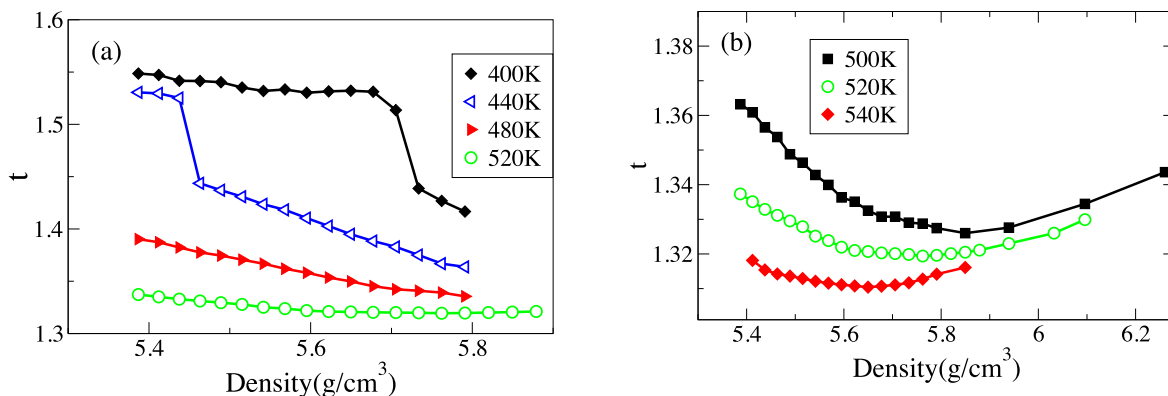


FIG. 4. Structural properties of liquid gallium. (a) The translational order parameter  $t$  as a function of density along isotherms. The discontinuity in  $t$  for  $T < 450$  K corresponds to a first-order LLPT, from LDL to HDL. In the one phase region at higher temperature  $t$  is continuous. (b) Structural anomaly: translational order  $t$  exhibits a minimum for temperature ranging from 460 K to 560 K, indicative of structural anomaly along each isotherm.

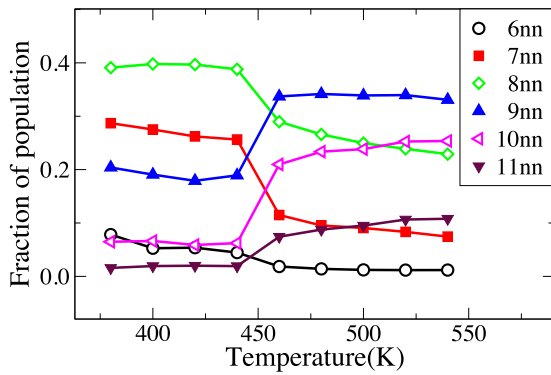


FIG. 5. The fraction of atoms with different number of nearest neighbors at different temperature for  $P = -2$  GPa. Atoms are classified based on the number of their nearest neighbors (nn). As temperature decreases, the population of atoms with  $nn < 9$  increases, while it decreases for  $nn \geq 9$  when local orientational symmetry is more similar to the LDL.

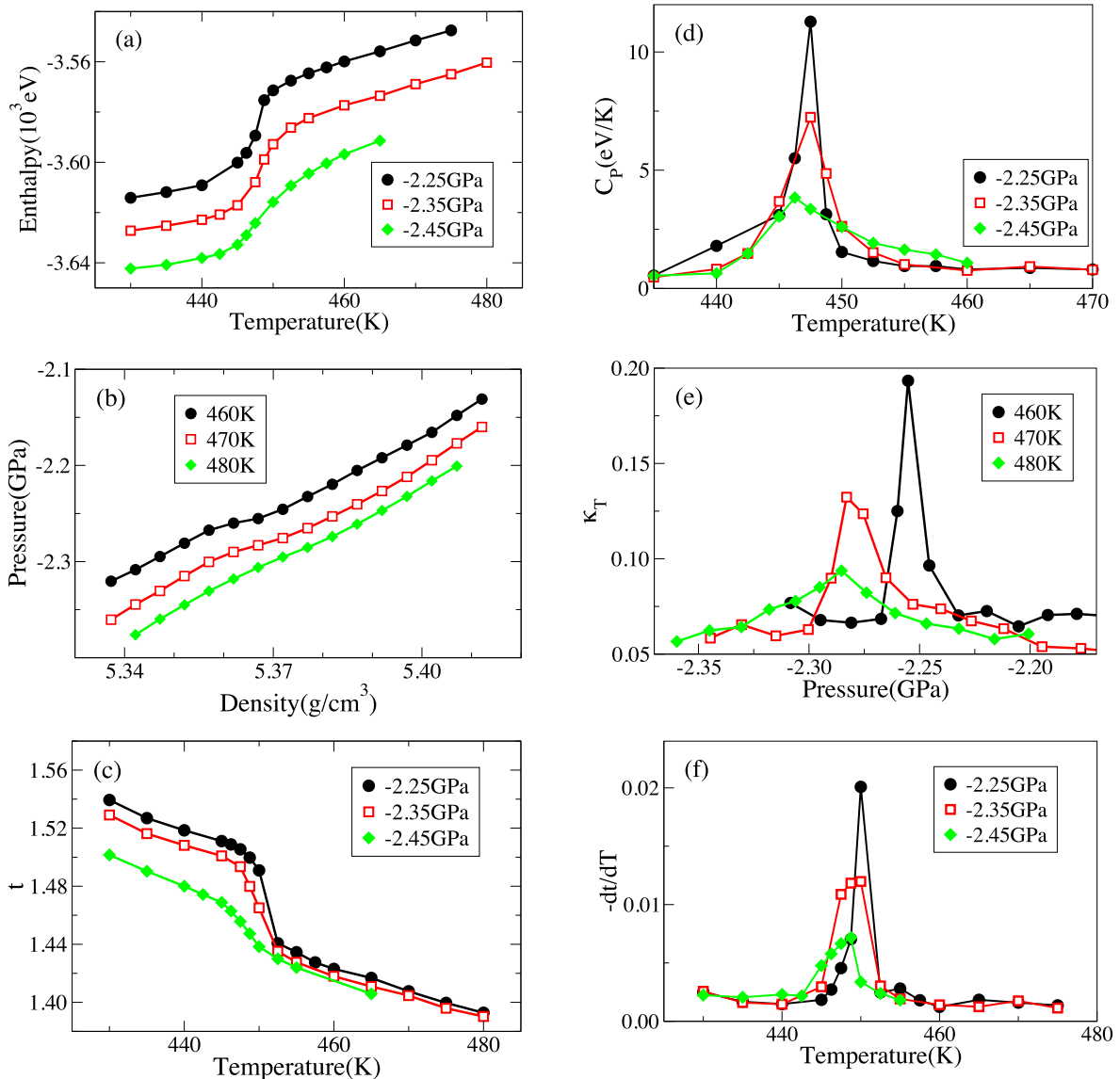


FIG. 6. State function and response function beyond the LLCP in supercritical region. (a) Enthalpy  $H$  as a function of temperature, (b) density as a function of pressure, (c) and structural order  $t$  as a function of temperature along isobar. The response functions (d)-(f),  $C_P$ ,  $\kappa_T$ , and the derivative of structural order  $dt/dT$ , show maxima along constant pressure or constant temperature paths. The magnitude of these response function maxima becomes sharper and sharper as the liquid-liquid critical temperature or pressure is approached.

as enthalpy  $H$  [Fig. 6(a)] and density  $\rho$  [Fig. 6(b)], change continuously along constant pressure or constant temperature paths below the LLCP. The corresponding response functions show maxima, e.g., specific heat  $C_P = (\frac{\Delta H}{\Delta T})_P$  at  $T_{max}(P)$  [Fig. 6(d)] and isothermal compressibility  $\kappa_T = -\frac{1}{V}(\frac{\Delta V}{\Delta P})_T$  at  $P_{max}(T)$  [Fig. 6(e)]. In addition, as the critical point is approached, the magnitude of response function maximum becomes sharper and sharper.

We note that the response function of structural order  $t$ , defined as the derivative of  $t$  [Fig. 6(c)], also shows maxima upon cooling along constant pressures [Fig. 6(f)], similar as that of  $\kappa_T$  and  $C_P$ . The loci of these response function maxima, presented in Figure 1, asymptotically converge to one line called the Widom line in the vicinity of the LLCP.<sup>12</sup> The Widom line is considered as the extension of the liquid-liquid coexistence line in the supercritical region. This is because the liquid structures at high and low temperature



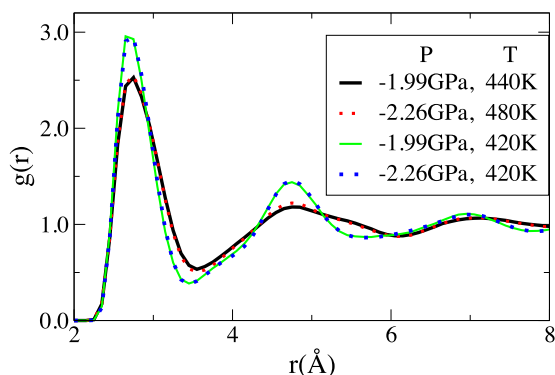


FIG. 7. Pair correlation function  $g(r)$  for gallium. The structure upon crossing the coexistence line and the Widom line is similar, from HDL ( $P = -1.99$  GPa,  $T = 440$  K) to LDL ( $P = -1.99$  GPa,  $T = 420$  K) for the former and HDL-like ( $P = -2.26$  GPa,  $T = 480$  K) to LDL-like ( $P = -2.26$  GPa,  $T = 420$  K) for the latter case.

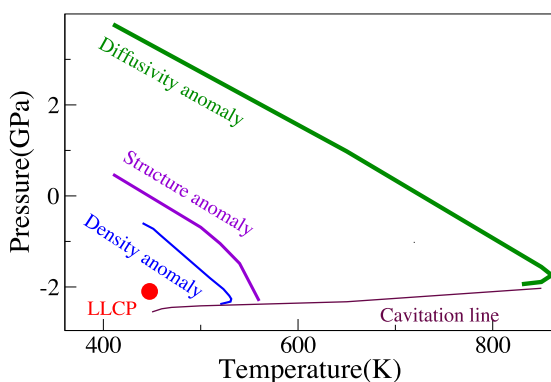


FIG. 8. The anomalous region of liquid gallium in the P-T phase diagram. The region of structural anomaly includes the region of density anomaly and is in turn encompassed by diffusivity anomaly region.

side of the Widom line are similar to that of the coexistence line [Fig. 7]. For instance, the pair correlation function  $g(r)$  at high and low temperature side of the Widom line (HDL-like for  $P = -2.26$  GPa and  $T = 480$  K and LDL-like for  $P = -2.26$  GPa and  $T = 420$  K) is almost the same as that of the liquid-liquid coexistence line (HDL for  $P = -1.99$  GPa and  $T = 440$  K and LDL for  $P = -1.99$  GPa and  $T = 420$  K), respectively [Fig. 7]. Such a supercritical phenomenon is consistent with that reported in water-like substances<sup>8–11</sup> and also provides a way to trace the LLPT and LLC of gallium from the supercritical region.

#### IV. SUMMARY

A number of substances predicted to have LLPT, such as water, silica, and germanium, exhibit water-like anomalies. Gallium was also reported to have two liquid states, however, whether it exhibits water-like anomalies is not yet studied. Using molecular dynamics simulations, we therefore investigate the phase behavior as well as its thermodynamic, dynamic, and structural properties of gallium. We find that liquid gallium has negatively sloped liquid-liquid coexistence line, similar to that of water. In particular, gallium exhibits density anomaly, diffusivity anomaly, and structural

anomaly, similar to substances with a predicted LLPT.<sup>8–11</sup> The anomalous regions are presented in the P-T phase diagram shown in Figure 8. It is found that the diffusivity anomaly region encloses that of structural anomaly, and the density anomaly region is enclosed inside that of the structure anomaly, which is different from that in water<sup>5,46</sup> and the model of Jagla liquid.<sup>44,47</sup> In the case of SPC/E and TIP5P water with negatively sloped liquid-liquid coexistence line, the region of diffusivity anomaly encloses the region of density anomaly, and the region of structural anomaly encompasses both diffusivity anomaly and density anomaly.<sup>5</sup> In the case of the model of Jagla liquid, two repulsive scale ramp potential<sup>47</sup> shows the same result with the case of SPC/E. But “two-scale” Jagla ramp potential with attractive and repulsive ramps shows the different result, with positively sloped liquid-liquid coexistence line, the region of density anomaly encompasses the diffusivity anomaly.<sup>44</sup>

In addition, we also find that the response functions of volume, enthalpy, and translational order parameter are continuous and show maxima in the supercritical region, the loci of which asymptotically approach to the other and merge to the Widom line.<sup>18</sup> This study thus provides a way to locate the LLC of gallium from high temperatures in the supercritical region. Since the chemical properties of gallium are very different from that of other substances having a LLC, our study indicates that anomalous behaviors may be a general feature for substances predicted to have the LLPT.

#### ACKNOWLEDGMENTS

We thank Dr. Xinggao Gong, Dr. Maozhi Li, and Dr. Weihua Wang for their helpful discussions. This work is supported by the National Basic Research Program of China 973 Program (Grant Nos. 2012CB921404 and 2015CB856801) and National Natural Science Foundation of China (NSFC Grant Nos. 11290162 and 11525520). We are also grateful for computational resources provided by the supercomputer TianHe-1A in Tianjin, China.

<sup>1</sup>P. H. Poole, F. Sciortino, U. Essmann, and H. E. Stanley, *Nature* **360**, 324 (1992).

<sup>2</sup>Y. Katayama, T. Mizutani, W. Utsumi, O. Shimomura, M. Yamakata, and K. Funakoshi, *Nature* **403**, 170 (2000).

<sup>3</sup>S. Sastry and C. Austen Angell, *Nat. Mater.* **2**, 739 (2003).

<sup>4</sup>I. Saika-Voivod, F. Sciortino, and P. H. Poole, *Phys. Rev. E* **63**, 011202 (2000).

<sup>5</sup>J. R. Errington and P. G. Debenedetti, *Nature* **409**, 318 (2001).

<sup>6</sup>M. S. Shell, P. G. Debenedetti, and A. Z. Panagiotopoulos, *Phys. Rev. E* **66**, 011202 (2002).

<sup>7</sup>V. V. Vasisht, J. Mathew, S. Sengupta, and S. Sastry, *J. Chem. Phys.* **141**, 124501 (2014).

<sup>8</sup>C. A. Angell, J. Shuppert, and J. C. Tucker, *J. Phys. Chem.* **77**, 3092 (1973).

<sup>9</sup>R. J. Speedy and C. A. Angell, *J. Chem. Phys.* **65**, 851 (1976).

<sup>10</sup>P. Kumar and H. E. Stanley, *J. Phys. Chem. B* **115**, 14269 (2011).

<sup>11</sup>F. Corsetti, E. Artacho, J. M. Soler, S. S. Alexandre, and M. V. Fernandez-Serra, *J. Chem. Phys.* **139**, 194502 (2013).

<sup>12</sup>S. Sastry, P. G. Debenedetti, F. Sciortino, and H. E. Stanley, *Phys. Rev. E* **53**, 6144 (1996).

<sup>13</sup>J. S. Tse and D. D. Klug, *Phys. Chem. Chem. Phys.* **14**, 8255 (2012).

<sup>14</sup>T. Limmer and D. Chandler, *J. Chem. Phys.* **135**, 134503 (2011).

<sup>15</sup>J. C. Palmer, F. Martelli, Y. Liu, R. Car, A. Z. Panagiotopoulos, and P. G. Debenedetti, *Nature* **510**, 385 (2014).

<sup>16</sup>J. A. Sellberg, C. Huang, T. A. McQueen, N. D. Loh, H. Laksmono, D. Schlesinger, R. G. Sierra, D. Nordlund, C. Y. Hampton, D. Starodub, D.

- P. DePonte, M. Beye, C. Chen, A. V. Martin, A. Barty, K. T. Wikfeldt, T. M. Weiss, C. Caronna, J. Feldkamp, L. B. Skinner, M. M. Seibert, M. Messerschmidt, G. J. Williams, S. Boutet, L. G. M. Pettersson, M. J. Bogan, and A. Nilsson, *Nature* **510**, 381 (2014).
- <sup>17</sup>C. A. Angell, *Science* **319**, 582 (2008).
- <sup>18</sup>L. Xu, P. Kumar, S. V. Buldyrev, S. H. Chen, P. H. Poole, F. Sciortino, and H. E. Stanley, *Proc. Natl. Acad. Sci. U. S. A.* **102**, 16558 (2005).
- <sup>19</sup>P. H. Poole, I. S. Voivod, and F. Sciortino, *J. Phys.: Condens. Matter* **17**, L43 (2005).
- <sup>20</sup>K. Murata and H. Tanaka, *Nat. Mater.* **11**, 436 (2012).
- <sup>21</sup>D. A. Fuentesvilla and M. A. Anisimov, *Phys. Rev. Lett.* **97**, 195702 (2006).
- <sup>22</sup>L. Liu, S. H. Chen, A. Faraone, C. W. Yen, and C. Y. Mou, *Phys. Rev. Lett.* **95**, 117802 (2005).
- <sup>23</sup>L. Xu, F. Mallamace, Z. Yan, F. W. Starr, S. V. Buldyrev, and H. E. Stanley, *Nat. Phys.* **5**(8), 565-569 (2009).
- <sup>24</sup>M. A. Morales, C. Pierleoni, E. Schwegler, and D. M. Ceperley, *Proc. Natl. Acad. Sci. U. S. A.* **107**, 12799 (2010).
- <sup>25</sup>M. A. Morales, J. M. McMahon, C. Pierleoni, and D. M. Ceperley, *Phys. Rev. Lett.* **110**, 065702 (2013).
- <sup>26</sup>R. Li, J. Chen, X. Li, E. Wang, and L. Xu, *New J. Phys.* **17**(6), 063023 (2015).
- <sup>27</sup>G. N. Greaves, M. C. Wilding, S. Fearn, D. Langstaff, F. Kargl, S. Cox, Q. V. Van, O. Majerus, C. J. Benmore, R. Weber, C. M. Martin, and L. Hennen, *Science* **322**, 566 (2008).
- <sup>28</sup>M. I. Baskes, S. P. Chen, and F. J. Cherne, *Phys. Rev. B* **66**, 104107 (2002).
- <sup>29</sup>O. Schulte and W. B. Holzapfel, *Phys. Rev. B* **55**, 8122 (1997).
- <sup>30</sup>K. Kadau, F. J. Cherne, R. J. Ravelo, and T. C. Germann, *Phys. Rev. B* **88**, 144108 (2013).
- <sup>31</sup>D. Sheppard, S. Mazevet, F. J. Cherne, R. C. Albers, K. Kadau, T. C. Germann, J. D. Kress, and L. A. Collins, *Phys. Rev. E* **91**, 063101 (2015).
- <sup>32</sup>X. G. Gong, G. L. Chiarotti, M. Parrinello, and E. Tosatti, *Phys. Rev. B* **43**, 14277 (1991).
- <sup>33</sup>X. G. Gong, G. L. Chiarotti, M. Parrinello, and E. Tosatti, *Europhys. Lett.* **21**, 469 (1993).
- <sup>34</sup>X. G. Gong and E. Tosatti, *Phys. Lett. A* **166**, 369 (1992).
- <sup>35</sup>C. Tien, E. V. Charnaya, W. Wang, Y. A. Kumzerov, and D. Michel, *Phys. Rev. B* **74**, 024116 (2006).
- <sup>36</sup>D. A. C. Jara, M. F. Michelon, A. Antonelli, and M. de Koning, *J. Chem. Phys.* **130**, 221101 (2009).
- <sup>37</sup>S. Cajahuaranga, M. de Koning, and A. Antonelli, *J. Chem. Phys.* **136**, 064513 (2012).
- <sup>38</sup>M. C. Rose and R. E. Cohen, *Phys. Rev. Lett.* **109**, 187604 (2012).
- <sup>39</sup>J. P. Perdew, *Phys. B: Condens. Matter* **172**, 1 (1991).
- <sup>40</sup>M. I. Baskes, *Phys. Rev. B* **46**, 2727 (1992).
- <sup>41</sup>E. A. Brandes, in *Smithells Metals Reference Book* (Butterworths, London, 1983).
- <sup>42</sup>E. B. Amitin, Y. F. Minenkov, O. A. Nabutovskaya, I. E. Paukov, and S. I. Sokolova, *J. Chem. Thermodyn.* **16**, 431 (1984).
- <sup>43</sup>S. Plimpton, *J. Comput. Phys.* **117**, 1 (1995).
- <sup>44</sup>L. Xu, S. V. Buldyrev, C. A. Angell, and H. E. Stanley, *Phys. Rev. E* **74**, 031108 (2006).
- <sup>45</sup>P. Gallo and F. Sciortino, *Phys. Rev. Lett.* **109**, 177801 (2012).
- <sup>46</sup>Z. Yan, S. V. Buldyrev, P. Kumar, N. Giovambattista, P. G. Debenedetti, and H. E. Stanley, *Phys. Rev. E* **76**, 051201 (2007).
- <sup>47</sup>Z. Yan, S. V. Buldyrev, N. Giovambattista, and H. E. Stanley, *Phys. Rev. Lett.* **95**, 130604 (2005).